Histochem Cell Biol (2009) 131:103–114
DOI 10.1007/s00418-008-0475-y

ORIGINAL PAPER

Caveolae in fibroblast-like synoviocytes: static structures associated with vimentin-based intermediate filaments

Kasper D. Berg · Raluca M. Tamas · Anne Riemann · Lise-Lotte Niels-Christiansen · Gert H. Hansen · E. Michael Danielsen

Accepted: 30 June 2008 / Published online: 22 July 2008

Abstract The fibroblast-like synoviocyte is a CD13-positive cell-type containing numerous caveolae, both single and interconnected clusters. In unstimulated cells, all single caveolae at the cell surface and the majority of those localized deeper into the cytoplasm were freely accessible from the medium, as judged from electron microscopy of synoviocytes exposed to the membrane impermeable marker Ruthenium Red. Caveolar internalization could be induced by a CD13 antibody or by cholera toxin B subunit (CTB). Thus, in experiments using sequential labeling with Alexa 488- and 594-conjugated CTB, about 50% of CTB-positive caveolae were internalized by 5 min of chase, and these remained inaccessible from the cell surface for periods up to 24 h. No colocalization with an endosomal marker, EEA1, or Lysotracker was observed, indicating that internalized caveolae clusters represent a static compartment. Vimentin was identified as the most abundant protein in detergent resistant membranes (DRM's), and by immunogold electron microscopy caveolae were seen in intimate contact with intermediate-size filaments. These observations indicate that vimentin-based filaments are responsible for the spatio-temporal fixation of caveolae clusters. RECK, a glycosylphosphatidylinositol-anchored protein acting as a negative regulator of cell surface metalloproteinases, was also localized to the caveolae clusters. We propose that these clusters function as static reservoirs of specialized lipid raft domains where proteins involved in cell–cell interactions, such as CD13, can be sequestered by binding to RECK in a regulatory manner.

Keywords Caveolae · Caveolin · Cholera toxin B · CD13 · RECK · Vimentin · Endocytosis

K. D. Berg · R. M. Tamas · A. Riemann · L.-L. Niels-Christiansen · G. H. Hansen · E. Michael Danielsen (✉)
Department of Cellular and Molecular Medicine,
The Panum Institute, Building 6.4, Blegdamsvej 3,
2200 Copenhagen N, Denmark
e-mail: midan@imbg.ku.dk

Present Address:
R. M. Tamas
Biochemistry and Cell Biology Program,
School of Engineering and Science, Jacobs University of Bremen,
Campus Ring 1, 28759 Bremen, Germany

Present Address:
A. Riemann
Julius-Bernstein-Institut für Physiologie,
Martin-Luther-Universität, Halle, Germany

Introduction

Caveolae were discovered by electron microscopy as small (60–80 nm) flask-shaped plasmalemma vesicles more than 50 years ago (Palade 1953; Yamada 1955). They are particularly abundant in adipocytes, smooth muscle cells, endothelial cells and fibroblasts and reportedly function in a multitude of cellular transport- and signaling processes (Mineo and Anderson 2001; Nichols and Lippincott-Schwartz 2001; Pelkmans and Helenius 2003; Carver and Schnitzer 2003; Hommelgaard et al. 2005; Parton and Simons 2007; Patel et al. 2008). Caveolae owe the characteristic shape to their main structural proteins, the caveolins (Fra et al. 1995; Drab et al. 2001). These are ~22 kDa cholesterol-binding proteins with both the N- and C-terminal ends in the cytoplasm and anchored to the membrane by a central putative hairpin intramembrane domain. About 150 oligomerized caveolin molecules are present in a single caveola (Williams and Lisanti 2004; Pelkmans and Zerial 2005) which has also been estimated to harbor ~20,000 cholesterol molecules and to be relatively enriched in

certain sphingoglycolipids and sphingomyelin (Ortegren et al. 2004). This composition favors the formation of liquid-ordered lipid raft domains, and caveolins and other proteins that localize to caveolae are generally found to be enriched in preparations of detergent resistant membranes (DRM's) (Simons and Ikonen 1997; Anderson 1998).

Assembly of caveolae de novo is thought to take place in the secretory pathway, most likely in a late Golgi compartment from where they are subsequently targeted to the plasma membrane as exocytotic caveolar carriers (Parton and Simons 2007; Echarri et al. 2007). Their mode of functioning at the surface of various types of cells has been intensely studied for several years, but it is still a matter of some controversy whether they are static or dynamic membrane structures. Early on, the term potocytosis was introduced to describe a receptor-mediated endocytosis of folate by caveolae, followed by direct delivery to the cytoplasm and thus bypassing the lysosomes (Anderson et al. 1992). However, experiments including FRAP microscopy of cells expressing GFP-caveolin-1 later indicated that caveolae remain at the cell surface as immobile units for long periods of time (Thomsen et al. 2002). More recently, TIR-FM experiments have revealed two possible modes of dynamic caveolar functioning in HeLa cells: one consisting of rapid fission–fusion cycles taking place in close vicinity of the plasma membrane (termed kiss-and-run recycling), and another, microtubule-dependent long-range cytoplasmic transport (Pelkmans and Zerial 2005). Furthermore, caveolar mobility and long-range transport to caveosomes could be dramatically increased by simian virus 40 (SV40) (Tagawa et al. 2005), a virus known to use caveolae for cell entry (Anderson et al. 1996). In either mode, however, the caveolae function as fixed entities, i.e., unlike clathrin- and COP-mediated vesicular transport, where coat molecules undergo cycles of assembly and disassembly.

Fibroblast-like synoviocytes are rich in caveolae, both single and interconnected in large clusters, and in a previous work the membrane peptidase CD13 (also known as aminopeptidase N) was shown to reside partially in clusters in the "flat" areas of the plasma membrane and partially in caveolae (Riemann et al. 2001). CD13 is an ectopeptidase that has been implicated in the control of growth and differentiation of many cellular systems, and it is involved in processing a number of peptide hormones, including angiotensins, met-enkephalin, and somatostatin (Riemann et al. 1999). In addition, it has been proposed to function together with CD64 (Fcγ receptor) in a multimeric receptor complex in monocytes (Riemann et al. 2005), and to act as a modulator of signal transduction and cell motility in endothelial cells (Petrovic et al. 2007). Furthermore, human coronavirus 229E exploits CD13 as a receptor and causes a redistribution of the peptidase from the surface to caveolae in fibroblasts (Nomura et al. 2004), and recently CD13 was reported to be regulated by the reversion-inducing cysteine-rich protein with Kazal motifs (RECK) by a modulation of its surface expression (Miki et al. 2007).

To gain more insight into caveolar functioning, we here studied the accessibility of synoviocyte caveolae from the cell surface in unstimulated cells as well as during the internalization of CD13 and cholera toxin B subunit (CTB). We found that all single caveolae and most but not all of the caveolae clusters are normally freely accessible. About 50% of all caveolae were capable of internalizing CTB within 5 min of chase, but once internalized, the toxin remained in the closed caveolae for periods up to 24 h, as judged by lack of colocalization with markers for endosomes (EEA1) and lysosomes (lysotracker). The synoviocyte caveolae clusters were strongly associated with vimentin-based intermediate filaments, and we propose that association with this cytoskeleton without molecular motors for vesicle trafficking attached, may explain the static behavior of caveolae in synoviocytes and other cell types. Finally, RECK localized to the caveolae clusters and by associating with CD13 may act to down regulate the expression of the proteinase at the "open" cell surface.

Materials and methods

Materials

Reagents were obtained from the following commercial suppliers: Cholera toxin B subunit (CTB) and Ruthenium Red from Sigma–Aldrich (http://www.sigma-aldrich.com/), cholera toxin B subunit-Alexa Flour 488/594, Alexa Flour 488/594-conjugated secondary antibodies, LysoTracker®, Alexa Fluor 488 phalloidin, mouse anti-bovine α-tubulin, and MEM + Glutamax™ medium from Invitrogen (http://www.invitrogen.com/), mouse anti-human CD13 (aminopeptidase N), rabbit anti-human caveolin, and 8-well poly-lysine-coated culture slides from BD Pharmingen (http://www.bdbiosciences.com/), rabbit anti-human RECK (reversion-inducing-cysteined-rich protein), early endosome antigen 1 (EEA1) and mouse anti-pig vimentin from Santa Cruz Biotechnology (http://www.scbt.com/), and antifade mounting media and goat anti-mouse IgG from Dako (http://www.dako.com).

Isolation and culture of cells

The isolation of the fibroblast-like synoviocytes used was described previously (Schwachula et al. 1994; Riemann et al. 2001). Briefly, the cells were obtained from collagenase-dispersed synovectomy tissues of patients suffering from juvenile chronic arthritis or rheumatoid arthritis, and grown on cover slides in MEM + Glutamax™ medium, containing 10% fetal calf serum and antibiotics. Cells were

passaged with 0.2 mM EDTA and 0.05% trypsin, and experiments were performed using cells of the fourth to the fifteenth passages. The cells were a homogeneous population of fibroblasts not positive for the macrophage-specific antigens CD14 and CD68.

Electron microscopy

Surface-labeling experiments with the electron dense membrane impermeable marker Ruthenium Red were performed with cells as follows: After a 5 min wash in 0.1 M sodium cacodylate, pH 7.2, the cells were fixed in 2.5% glutaraldehyde and 0.05% Ruthenium Red in the above buffer for 1 h. The cells were then washed three times for 10 min in the cacodylate buffer and post fixed for 1 h with 1% Osmium tetroxide containing 0.05% Ruthenium Red. After three washes for 10 min in cacodylate buffer, followed by three washes in water, the cells were dehydrated and finally embedded in Epon as previously described (Hansen et al. 1984).

Immunogold labeling of vimentin was performed as previously described (Hansen et al. 1992). Ultrathin Epon sections were etched in 1% H_2O_2 in water for 5 min and then treated in a series of droplets as follows: (a) 50 mM Tris–HCl, 150 mM NaCl, 1% Triton X-100, pH 7.4 (TBS) for 3× 10 min; (b) 3% bovine serum albumin in 20 mM Tris–HCl, 150 mM NaCl, 0.25% bovine serum albumin, 1% Triton X-100, pH 8.2 (gold buffer) for 30 min; (c) vimentin antibody (diluted 1:50 in gold buffer) overnight at 4°C and for 1 h at 20°C; (d) gold buffer for 3× 10 min; (e) goat anti-mouse IgG conjugated to 13 nm gold particles diluted in gold buffer for 30 min; (f) gold buffer for 3× 10 min; (g) TBS for 2× 5 min; (h) water for 2× 5 min. The sections were finally contrasted in 1% uranyl acetate in water for 5 min and in lead citrate for 30 s. Control experiments were performed in parallel with omission of the primary antibody.

The sections were examined in a Zeiss EM 900 electron microscope equipped with a Mega View II digital camera.

Immunofluorescence microscopy

For internalization studies of CD13, cells were washed twice for 5 min in TBS and then incubated at 4°C with CD13 antibodies (1:200 dilution) in TBS for 1 h in the presence or absence of CTB (10 μg/ml). After 2 washes for 5 min in TBS, the cells were incubated at 37°C for 1 h before fixation in 4% paraformaldehyde in sodium phosphate, pH 7.2 (PB) for 1 h. For visualization of CD13 at the surface, labeling with a secondary Alexa 488-conjugated antibody (diluted 1:200 in TBS) was performed for 30 min. After two washes in TBS, the cells were permeabilized for 2× 5 min in TBS containing 0.05% saponin and 0.02 M glycin. Then the cells were incubated for 30 min in TBS containing 0.05% saponin and 3% bovine serum albumin. For visualization of intracellular and surface-bound CD13, the cells were incubated for 30 min with a secondary Alexa 594-conjugated antibody (1:200 dilution in TBS containing 0,05% saponin and 0,25% bovine serum albumin) and finally the cells were washed 4× 5 min in TBS containing 0,05% saponin.

For colocalization of CD13 and RECK, surface double labeling was performed sequentially on cells fixed in 4% paraformaldehyde in PB for 1 h with primary antibodies (1:200 dilution), followed by incubation for 30 min with Alexa 488/594-conjugated secondary antibodies. For surface double labeling of RECK and CTB, the RECK labeling was performed first, as described above, followed by labeling with Alexa 488-conjugated CTB (10 μg/ml) for 1 h.

For surface labeling of CTB and caveolin 1, cells fixed in 4% paraformaldehyde in PB were labeled for 1 h with CTB-Alexa 594 (10 μg/ml). After washing and permeabilization with saponin as described above, the cells were labeled with an antibody to caveolin 1 (1:100 dilution), followed by incubation for 30 min with an Alexa 488 secondary antibody.

For internalization studies of CTB, cells were labeled for 10 min with CTB-Alexa 488 (10 μg/ml medium), washed briefly with medium and incubated at 37°C for periods of 0 min–24 h. In some experiments, the cells were then cooled to 4°C and incubated for 20 min at this temperature in the presence of CTB-Alexa 594 (10 μg/ml) for visualization of CTB localized at the cell surface, followed by fixation in 4% paraformaldehyde in PB for 1 h. For calculations of colocalization, the point method was used (Williams 1977). Each time point was based on analysis of 5–12 cells and 200–300 spots/cell were counted.

For colocalization of CTB and EEA-1, the cells were incubated at 37°C for 30 min with CTB-Alexa 488 (10 μg/ml), washed, fixed in 4% paraformaldehyde in PB and permeabilized by saponin as described above before incubation for 30 min with an EEA1 antibody (1:100 dilution), followed by labeling with an Alexa 594 secondary antibody. For colocalization of CTB and lysosomes, cells were incubated at 37°C for 3 h with CTB-Alexa 488 (10 μg/ml), and during the last 1 h of incubation, Lysotracker (100 nM) was added to the medium of the CTB labeled cells. After a brief wash, the cells were fixed in 4% paraformaldehyde in PB for 1 h and briefly washed in PB.

For visualization of cytoskeletal filaments, the cells were first fixed in 4% paraformaldehyde in PB and permeabilized by saponin as described above. Intermediate filaments and microtubules were then labeled by primary antibodies to vimentin and α-tubulin (1:200 dilution), respectively, followed by labeling with Alexa-conjugated secondary antibodies. Actin filaments were visualized by labeling for 30 min with Alexa 488-conjugated phalloidin (10 units/ml).

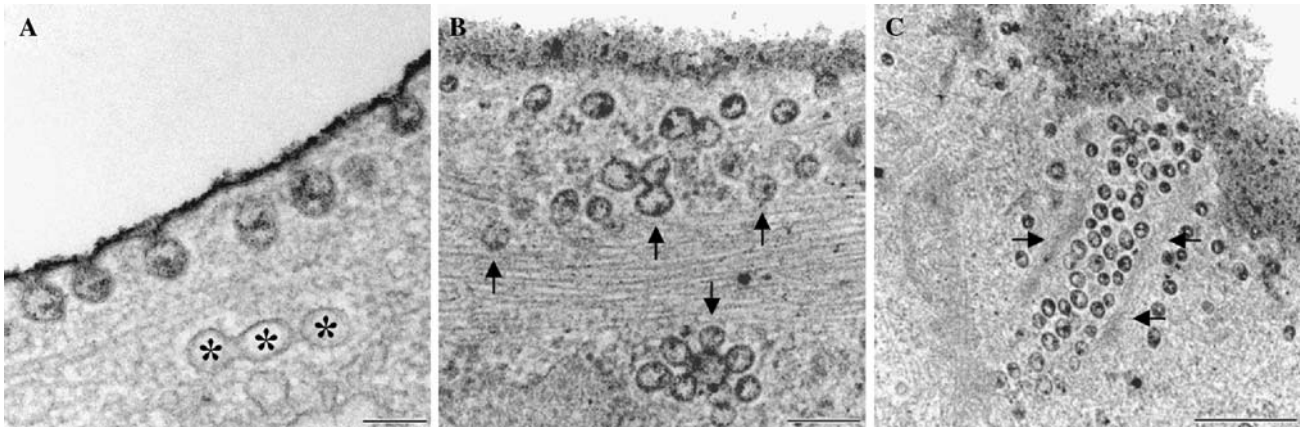

Fig. 1 Surface labeling with Ruthenium Red. Synoviocytes were fixed in the presence of the nonpermeable surface marker Ruthenium Red. The electron micrographs show the presence of numerous caveolae. Single caveolae are typically seen directly at the cell surface (**a**), whereas caveolae clusters are most often found deeper within the cell (**b**, **c**). Both types of caveolae were extensively stained by Ruthenium Red, and unstained caveolae (marked with *asterisks* in **a**) were only rarely observed. Intermediate-size (10 nm) cytoskeletal filaments (*arrows*) were frequently found in close contact with the caveolae clusters (**b**, **c**). *Bars* 0.1 μm (**a**), 0.2 μm (**b**), 0.5 μm (**c**)

In all antibody labeling experiments described above, controls with omission of the respective primary antibodies were included.

All labeled cells were finally washed for 2× 5 min in TBS and 2× 2 min in water, covered antifade in mounting medium and examined in a Leica DM 4000 B microscope equipped with a Leica DC 300 FX digital camera.

MALDI-TOF analysis

DRM's were prepared by sucrose gradient ultracentrifugation (Brown and Rose 1992) from synoviocytes extracted with 1% Triton X-100 as previously described (Danielsen 1995). After centrifugation, the sucrose gradient was divided into fractions that were subjected to SDS/PAGE and electrotransferred onto an Immobilon membrane. The most prominent band, of about 55 kDa, seen in the floating DRM fractions after staining with Coomassie Brilliant Blue, was carefully excised from the membrane and submitted to commercial MALDI-TOF analysis (Alphalyse, Odense, Denmark). A total of 12 different peptides were obtained, all corresponding to amino acid sequences of human vimentin.

Results

The majority of synoviocyte caveolae and caveolae clusters are freely accessible from the cell surface

In a previous study, synoviocytes were shown to be fibroblast-like cells with numerous caveolae (Riemann et al. 2001). These were seen both as single caveolae, mostly localized at, or close to, the cell surface, as well as large caveolae clusters often observed deeper into the cytoplasm. By pre-embedding immunogold electron microscopy, the surface membrane peptidase CD13 was shown to be present not only in the single caveolae at the cell surface but also in the deeper-lying caveolae clusters, indicating that at least some of the latter structures are freely accessible to the surface (Riemann et al. 2001). In addition, CD13 was also widely distributed in clusters over the noncaveolar part of the cell surface.

To study the caveolar surface connection in closer detail in the present work, cell labeling with the membrane impermeable marker Ruthenium Red was used for visualization of structures freely connected to the cell surface. As shown in Fig. 1, the majority of caveolae in the synoviocytes were labeled, indicating that they are exposed to the extracellular environment in the resting state. This was the case both for the single caveolae positioned close to the surface, as well as the clusters of interconnected caveolae typically seen deeper within the cell. However, among the many sections examined, unlabeled caveolae were only occasionally detected, indicating their ability to seal off from the surface (Fig. 1a). These unlabeled caveolae were most often of the clustered type and were always seen at some distance from the cell surface (Fig. 1b, c). In contrast, single caveolae seen in direct contact with the plasma membrane were always stained by Ruthenium Red, indicating a permanent access to the extracellular medium for this caveolar subpopulation. Overall, we estimate that >90% of the caveolae are in the "open" position in unstimulated cells.

Internalization of the surface membrane peptidase CD13

To detect internalization of the open caveolae and caveolae clusters harboring CD13, synoviocytes were surface

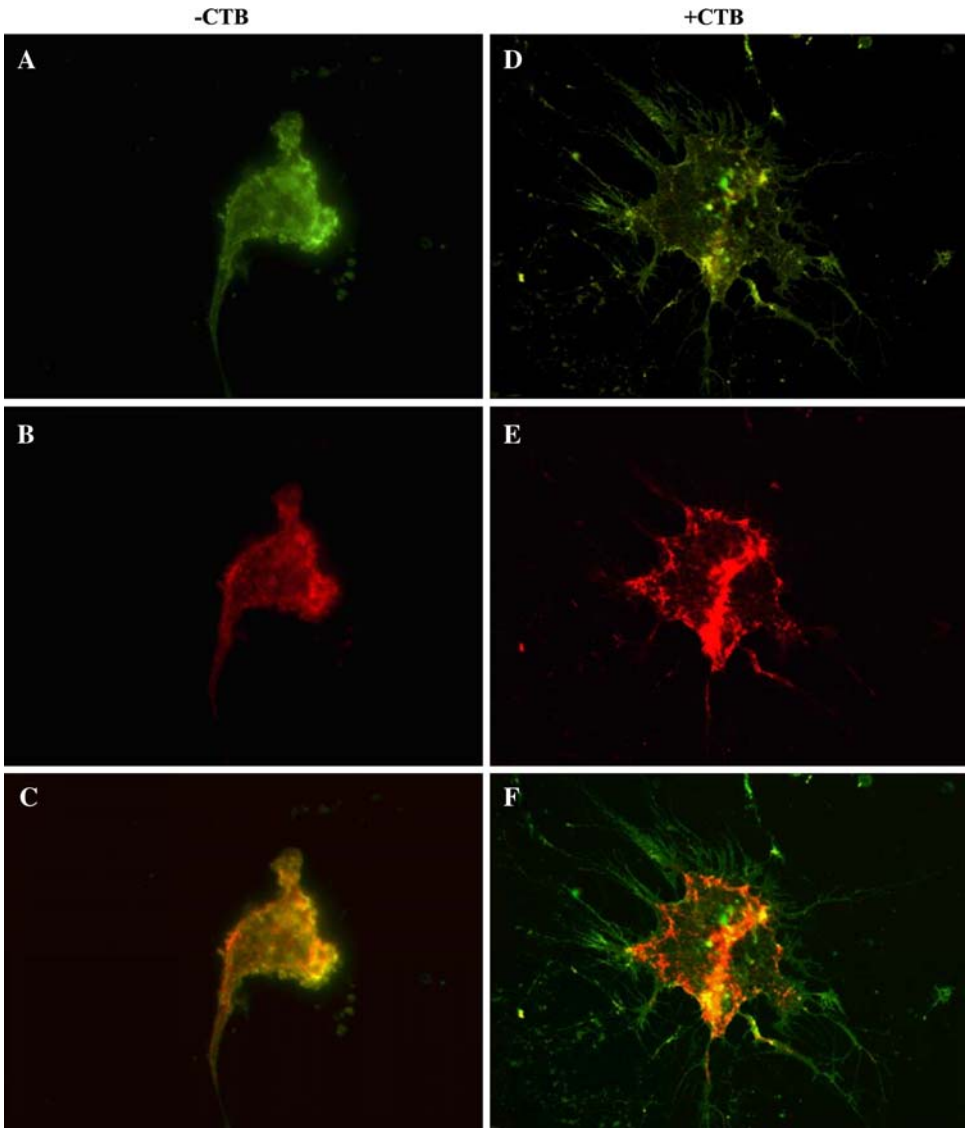

Fig. 2 Internalization of CD13. Synoviocytes were labeled with CD13 antibodies. After washing, the cells were incubated at 37°C for 1 h in the absence or presence of CTB. CD13 at the surface was then visualized by labeling with an Alexa 488-conjugated secondary antibody (**a**, **d**). After cell permeabilization with saponin, total (internalized and surface-localized) CD13 was detected by a second Alexa 594-conjugated secondary antibody (**b**, **e**). **c** and **f** The merged images. In the absence of CTB, few distinct punctae were only labeled after cell permeabilisation, indicating internalization of CD13. Addition of CTB greatly increased internalization

labeled at 4°C with a CD13 antibody, then incubated for 1 h at 37°C followed by fixation in 4% paraformaldehyde. The cells were then labeled with an Alexa 488-conjugated secondary antibody, then permeabilized by saponin, and finally labeled with an Alexa 594-conjugated secondary antibody to visualize also internalized CD13. The cell surface-labeling showed a weak, uniform distribution of CD13 at the non-caveolar part of the plasma membrane, as well as more intensely labeled punctae, representing single or clustered caveolae (Fig. 2a). A similar labeling was obtained by the second secondary antibody, but in addition some distinct punctae were only labeled after cell permeabilization, indicating an internalization of caveolae from the cell surface during the incubation at 37°C (Fig. 2b, c).

CTB is a toxin that specifically binds to ganglioside GM_1 at the surface of cells and has been widely used as a marker for lipid rafts and caveolae (Parton 1994; Orlandi and Fishman 1998; Sandvig and Van Deurs 2002; Parton and Richards 2003). When CTB was added during the 1 h incubation at 37°C in an experiment otherwise performed as the one described above, it markedly increased the internalization of CD13 (Fig. 2d–f), indicating that CTB and CD13 share a common mechanism of internalization.

From the above experiments we therefore conclude that although most caveolae/caveolae clusters in unstimulated synoviocytes are freely accessible from the surface, some are capable of being internalized from the cell surface when triggered by addition of the CD13 antibody and CTB.

Caveolar dynamics studied with CTB

As shown in Fig. 3, when fixed synoviocytes were incubated with fluorescent CTB, the toxin widely colocalized with caveolin, confirming that binding at the cell surface in synoviocytes preferentially takes place in single caveolae or caveolae clusters. To study the dynamics of caveolae

internalization, we performed sequential double color labeling experiments with Alexa 488- and Alexa 594-conjugated CTB (Fig. 4a). Colocalization of the two fluorophores was close to 90% when they were added simultaneously, but within 5 min of "chase" period between the two additions of toxin, colocalization decreased to about 45%, indicating the induction of a rapid internalization of about half the surface-bound CTB. During chase periods for up to 3 h, the degree of colocalization only slowly decreased further, to just under 30%. This degree of colocalization was observed even by 24 h of chase, indicating that the internalized CTB remains stable over a long period of time (Fig. 4b). Regardless of the chase time, the labeling representing internalized CTB was localized in punctae mainly centered around the nucleus, whereas the immobile, colocalized fraction was mainly seen at the periphery of the cell, in particular along the cell protrusions (Fig. 4a). This distribution agrees well with the Ruthenium Red experiments (Fig. 1), and implies the existence of an internalization-competent subpopulation of caveolae, consisting mainly of the caveolae clusters, and an immobile fraction of single caveolae in close proximity to the cell surface.

Stability of internalized caveolae

The sequential double labeling experiments presented above indicate a very long residence time for internalized CTB. To examine if some of the internalized CTB was transported to the endosomal system, a double labeling with CTB and EEA1, a marker for early endosomes (Mu et al. 1995), was performed, but as shown in Fig. 5, no colocalization between the two was detected after 30 min. Similarly, a double labeling with CTB and the lysosomal marker Lysotracker was performed, but again, no colocalization was observed after 3 h (Fig. 5). These results thus indicate that the internalized caveolae remain stationary and do not engage in trafficking to other compartments of the endo-lysosomal system.

Caveolae clusters organized by intermediate filaments

As shown in Fig. 1b, c, the caveolae clusters, in particular those localized at some distance from the cell surface, were frequently seen in close contact with dense bundles of cytoskeletal filaments. The association was not random; in many cases the caveolae were observed to align intimately along the filaments which had a diameter size of 10 nm. The filaments were immunogold labeled by an antibody to vimentin, demonstrating that they are of the intermediate type (Fig. 6a), and in higher magnification, putative linker proteins between filaments and caveolae were detectable (Fig. 6b). In line with this, the most abundant protein in DRM's prepared from synoviocytes, as judged from protein staining, was a 55-kDa band subsequently identified by MALDI-TOF analysis as vimentin (data not shown). That vimentin-based intermediate filaments are indeed abundant in synoviocytes, especially in the perinuclear region of the cell, is shown in Fig. 7. This figure also shows the distribu-

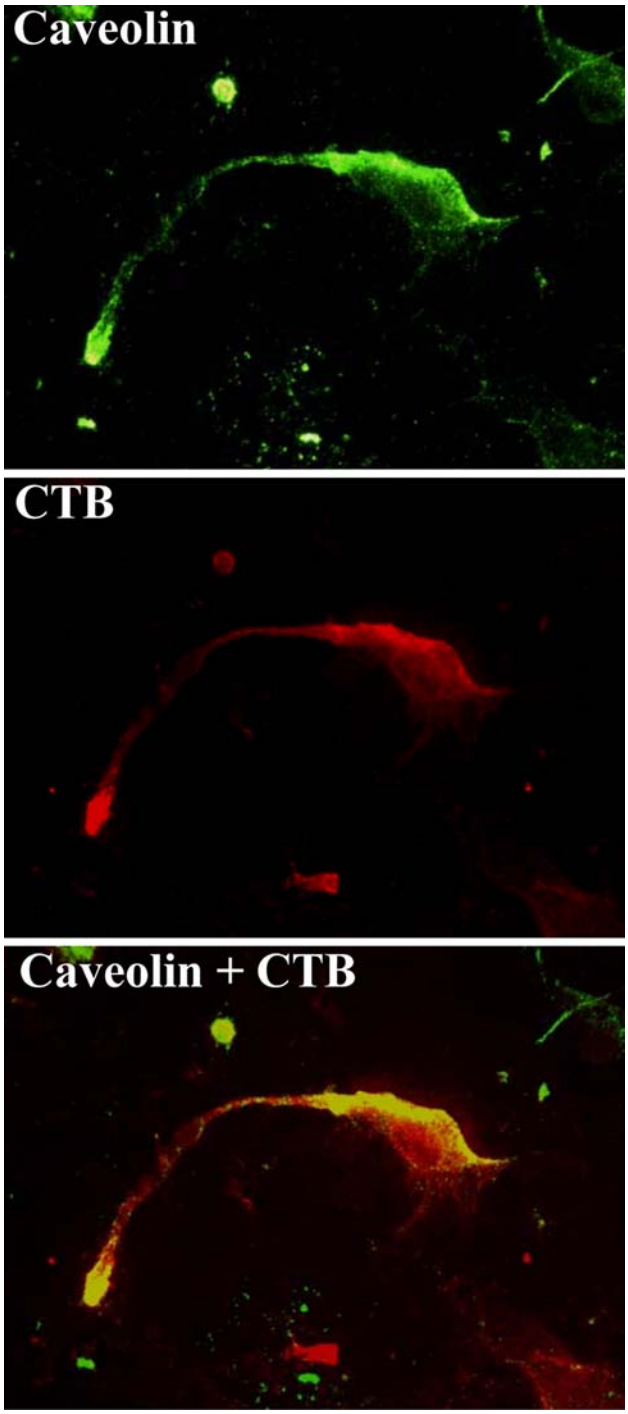

Fig. 3 Colocalization of caveolin and CTB. After fixation, synoviocytes were labeled for 1 h with Alexa 594-conjugated CTB. The cells were then washed, permeabilized and labeled with a caveolin 1 antibody, followed by labeling with an Alexa 488-conjugated secondary antibody. CTB and caveolin 1 were largely colocalized

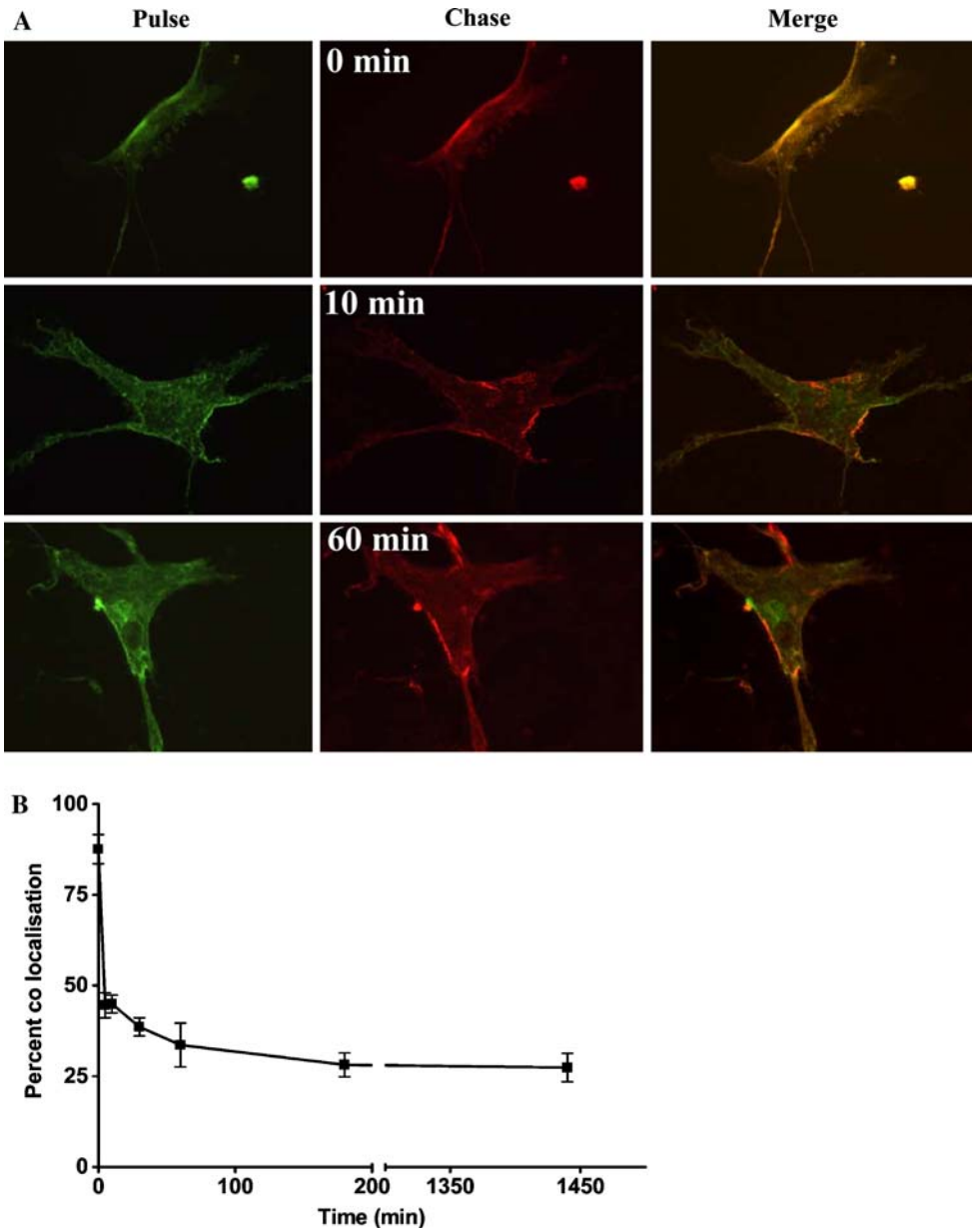

Fig. 4 Sequential dual color double labeling with CTB. **a** Synoviocytes were labeled for 10 min with Alexa 488-conjugated CTB. After washing, the cells were incubated at 37°C for the indicated periods of time before cooling to 4°C and labeling for 20 min with Alexa 594-conjugated CTB. The two CTB labelings largely colocalized at 0 min whereas distinct punctae of internalized CTB were seen both at 10 and 60 min. B: Graph showing the percentage colocalization of pulse- and chase labelings with incubation periods of 0 min–24 h. Each time point represents the mean (±SD) and is based on 5–12 cells where 200–300 spots/cell were counted

tion of the actin stress fibers and microtubules. In comparison with the spaghetti-like appearance of intermediate filaments, the stress fibers are more regular and uniformly organized, and the microtubules appear to concentrate particularly in areas active in filopodia formation.

Taken together, these experiments show that the elaborate caveolae cluster architecture relies on a scaffold provided by the intermediate filaments. Unlike actin—and microtubule filaments, intermediate filaments lack polarity and have no motor proteins associated with them, and for these reasons they are often perceived as scaffolding molecules designed mainly to provide structural stability to mechanical stress (Coulombe and Wong 2004; Styers et al. 2005). The strong caveolar association with this filament system may therefore provide an explanation of the extraordinary immobility of the internalized caveolae and the lack of trafficking to endosomes and lysosomes.

RECK localization in caveolae

RECK is a ubiquitously expressed glycosylphosphatidylinositol-anchored glycoprotein containing multiple serine protease inhibitor motifs that negatively regulates matrix metalloproteinase members (Noda and Takahashi 2007). Recently, RECK, a lipid raft protein, was reported to act by controlling the amounts of MT1-MMP as well as CD13 that associate with DRM's in transfected HT1080 cells, a human fibrosarcoma cell line (Miki et al. 2007). Figure 8 shows the distribution of RECK at the synoviocyte surface. Unlike the more widespread distribution of CD13, RECK

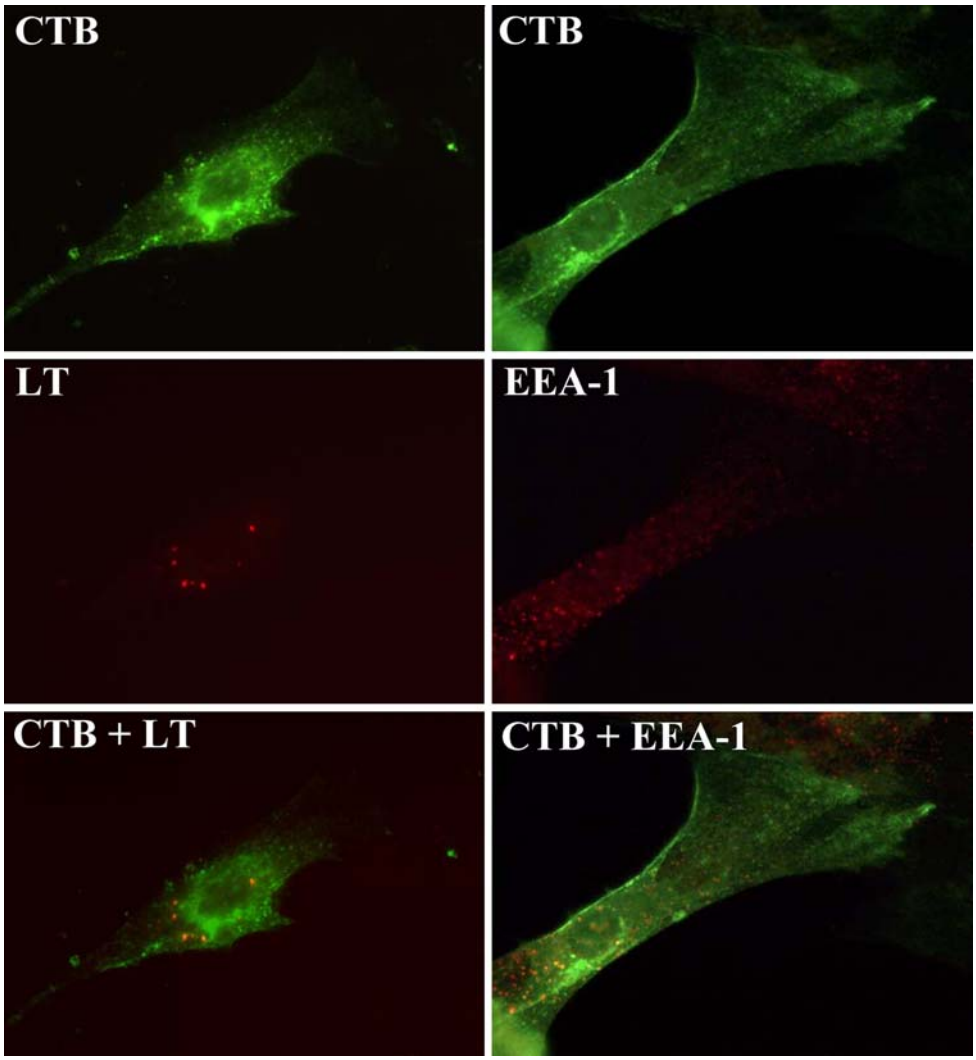

Fig. 5 Colocalization of CTB with EEA1 and Lysotracker. For colocalization with Lysotracker (*LT*), synoviocytes were incubated for 3 h at 37°C in the presence of Alexa 488-conjugated CTB. During the last 1 h of incubation, Alexa 594-conjugated Lysotracker was added to the culture medium. For colocalization with EEA1, synoviocytes were incubated for 30 min at 37°C in the presence of Alexa 488-conjugated CTB. After cooling to 4°C, the cells were fixed and permeabilized before labeling with an EEA1 antibody, followed by an Alexa 594-conjugated secondary antibody. No colocalization between CTB and either the early endosomal- or the lysosomal marker was observed

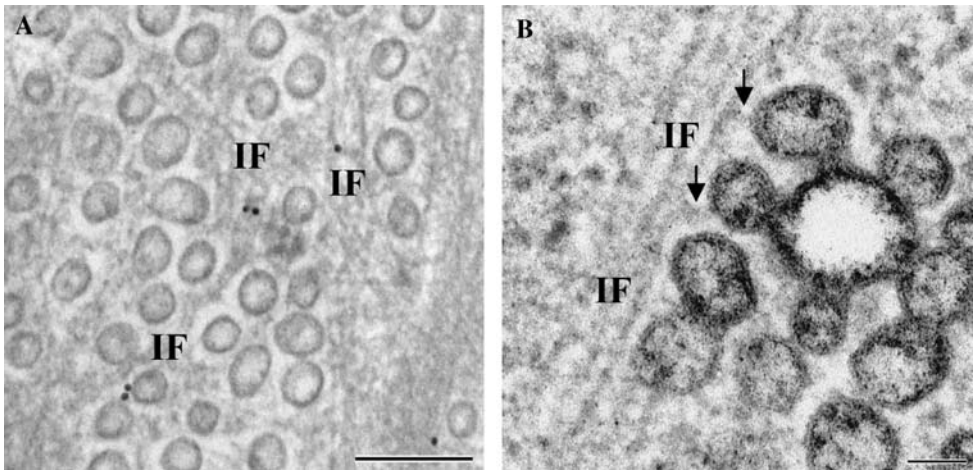

Fig. 6 Electron microscopy of caveolae-associated filaments. **a** Immunogold labeling of vimentin along intermediate-size filaments (IF) in close contact with caveolae. **b** A high magnification image of intermediate filaments (IF) and a Ruthenium Red stained caveolae cluster. Arrows indicate putative protein linker molecules between the filaments and the caveolae. *Bars* 0.1 μm (**a**), 0.05 μm (**b**)

has a distinct punctate localization concentrated around the central part of the cell with no or little labeling seen over the cellular protrusions. The RECK labeling partially colocalized with that of CTB, indicating that the double labeled punctae represent caveolae or caveolae clusters. Together, these experiments show that RECK is expressed in synoviocytes. In addition, given RECKs reported ability to interact directly with CD13, its localization in caveolae may enable it to prevent the latter protein from gaining access to the "open" noncaveolar part of the cell membrane.

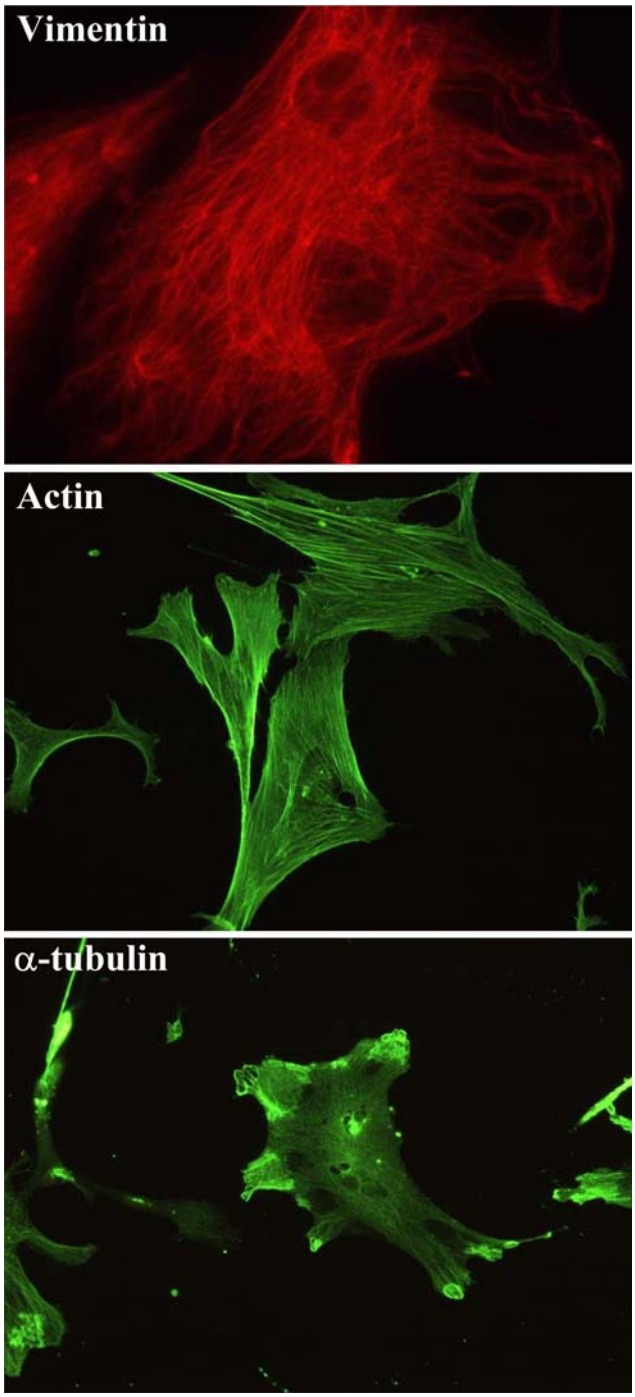

Fig. 7 Visualization of cytoskeletal filaments in synoviocytes. After fixation and permeabilization, synoviocytes were labeled with antibodies to either vimentin or a-tubulin followed by Alexa-conjugated secondary antibodies. For visualization of actin filaments, the permeabilized cells were labeled with Alexa 488-conjugated phalloidin. Each cytoskeletal system has its characteristic organization in synoviocytes

Discussion

The results obtained in the present work have revealed both some static and dynamic properties of caveolae and caveolae clusters in fibroblast-like synoviocytes. Thus, the electron microscopic cell surface analysis using Ruthenium Red demonstrated that the large majority of caveolar membranes in unstimulated cells are freely accessible to the extracellular medium. Furthermore, the infrequently occurring unlabeled caveolae were only detected in the subpopulation of caveolae that extend into the cytoplasm, suggesting that only these pleiomorphic membrane structures engage in internalization. In a study, using total internal reflection fluorescence microscopy methodology, single caveolae, as visualized by caveolin-1-GFP, were observed to undergo repeated and rapid (on a millisecond timescale) cycles of fission and fusion without disassembly of the caveolar coat (Pelkmans and Zerial 2005). Only 45% of the cell's caveolae engage in this apply termed kiss-and-run recycling which proceeds in a confined volume close to the cell surface and relies upon the activity of dynamin and a number of kinases. Assuming caveolar kiss-and-run occurs in a similar fashion in synoviocytes, caveolae thus engaged would be seen as static and, most likely, as open in the experiments with Ruthenium Red performed in the present work.

However, that caveolae in synoviocytes are capable of closure or internalization taking place on a much wider timescale was demonstrated by the sequential CTB labeling experiments. Here, about half the amounts of surface-bound CTB participated in this traffic, most likely induced to do so by clustering of the GM_1 receptors by the pentameric toxin. The kinetics of this process suggests that those caveolae capable of internalization do so rapidly (within 5 min of chase) and then remain surface inaccessible for a very long time (24 h). Morphologically, the internalization-competent caveolae were predominantly of the clustered type that extend deep into the cytoplasm. These so called endocytotic caveolar carriers (Parton and Simons 2007) may traffic further to either the endosomes (Sharma et al. 2003; Pelkmans et al. 2004) or the caveosomes reported previously by others to function as an intermediate compartment in caveolar endocytosis of SV40 as well as CTB (Pelkmans et al. 2001; Nichols 2002).

Clearly, the data obtained in the present work regarding further membrane transport of internalized CTB in synoviocytes do not fit well with the above dynamic concept of the caveosome as a major trafficking hub. The failure to detect a convincing colocalization with the endosomal marker EEA1 after 30 min or Lysotracker after 3 h of internalization strongly argues against a major pathway leading to the acidifying organelles. In fact, the persistence of the characteristic punctate labeling pattern throughout the time-course of the incubation suggests that most if not all internalized CTB in synoviocytes remains within the closed caveolar system. A possible explanation for this observed stability is the strong association with the intermediate filament system, as evidenced by the relative abundance of

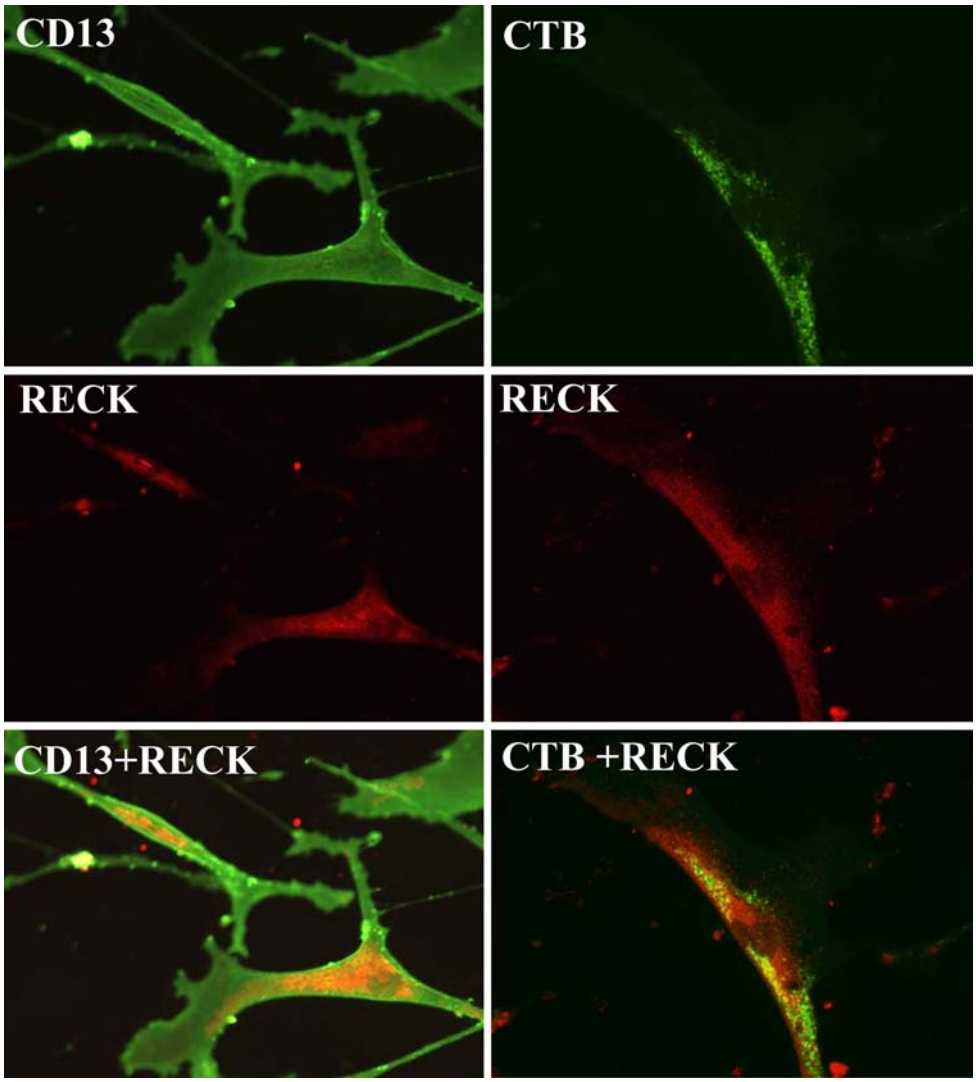

Fig. 8 Surface localization of RECK. After fixation, synoviocytes were labeled with an antibody to RECK, followed by an Alexa 594-conjugated secondary antibody. After washing, the cells were subsequently labeled with an antibody to CD13, followed by an Alexa 488-conjugated secondary antibody. Alternatively, the cells were labeled with Alexa 488-conjugated CTB after the labeling for RECK. Unlike the widespread localization of CD13, RECK labeling was confined to the central part of the cell. RECK partially colocalized with CTB, indicating that it is also present in caveolae

vimentin in synoviocyte DRM's, as well as by immunogold electron microscopy. Association between caveolae and intermediate filaments have previously been described for transmigrating endothelial cells (Santilman et al. 2007), but otherwise the action of the microfilaments has been implicated in caveolar endocytosis. Thus, SV40 binding in HeLa cells induced a transient break down of existing actin stress fibers and a recruitment of actin to virus-loaded caveolae to initiate formation of new actin fibers (Pelkmans et al. 2002). This ligand-triggered rearrangement of the actin cytoskeleton has been proposed to eliminate the spatial restrictions on caveolar dynamics and enable caveolae to switch from local kiss-and-run recycling to committed, long-range, microtubule-dependent internalization to intracellular organelles (Tagawa et al. 2005). The trafficking/functioning of caveolae in a given cell type therefore seems to depend upon their cytoskeletal interactions. Thus, in synoviocytes, where association with intermediate filaments dominates, we find it doubtful if the caveolae clusters that internalize CTB also engage in *bona fide* membrane trafficking from the surface to the cell interior. Conceivably, the internalization process may consist merely of a caveolar closure, taking place either at the cell surface or maybe somewhere within a pleiomorphic caveolae cluster. Furthermore, as judged by the experiments with Ruthenium Red, closure is a rare event in cells not challenged by pathogens and thus may not be an important part of normal caveolar functioning. This may be examplified by the dual localization of CD13, partly at "flat" areas of the plasma membrane and partly in caveolae. By sequestering from the former to the latter compartment by regulated association with the caveolar RECK protein (Miki et al. 2007), CD13 (and membrane proteinases of the MMP family) will be prevented from participating in cell–cell interactions and contact with the extracellular matrix regardless whether the caveolae are open or not. Along these lines, future work should aim to clarify which of the many other biological functions ascribed to caveolae, including signaling, lipid

regulation/storage and mechanosensing (Parton and Simons 2007) that involve true internalization.

Acknowledgments Karina Rasmussen is thanked for excellent technical assistance. The work was supported by grants from the Danish Medical Research Council and the Augustinus Foundation. R.M.T. and A.R. received traveling stipends from the Jacobs University, Bremen, Germany, and the European Union, respectively.

References

Anderson RG (1998) The caveolae membrane system. Annu Rev Biochem 67:199–225

Anderson RG, Kamen BA, Rothberg KG, Lacey SW (1992) Potocytosis: sequestration and transport of small molecules by caveolae. Science 255:410–411

Anderson HA, Chen Y, Norkin LC (1996) Bound Simian Virus 40 translocates to caveolin-enriched membrane domains, and its entry is inhibited by drugs that selectively disrupt caveolae. Mol Biol Cell 7:1825–1834

Brown DA, Rose JK (1992) Sorting of GPI-anchored proteins to glycolipid-enriched membrane subdomains during transport to the apical cell surface. Cell 68:533–544

Carver LA, Schnitzer JE (2003) Caveolae: mining little caves for new cancer targets. Nat Rev Cancer 3:571–581

Coulombe PA, Wong P (2004) Cytoplasmic intermediate filaments revealed as dynamic and multipurpose scaffolds. Nat Cell Biol 6:699–706

Danielsen EM (1995) Involvement of detergent-insoluble complexes in the intracellular transport of intestinal brush border enzymes. Biochemistry 34:1596–1605

Drab M, Verkade P, Elger M, Kasper M, Lohn M, Lauterbach B, Menne J, Lindschau C, Mende F, Luft FC, Schedl A, Haller H, Kurzchalia TV (2001) Loss of caveolae, vascular dysfunction, and pulmonary defects in caveolin-1 gene-disrupted mice. Science 293:2449–2452

Echarri A, Muriel O, Del Pozo MA (2007) Intracellular trafficking of raft/caveolae domains: insights from integrin signaling. Semin Cell Dev Biol 18:627–637

Fra AM, Williamson E, Simons K, Parton RG (1995) De novo formation of caveolae in lymphocytes by expression of VIP21-caveolin. Proc Natl Acad Sci USA 92:8655–8659

Hansen GH, Meier E, Schousboe A (1984) Gaba influences the ultrastructure composition of cerebellar granule cells during development in culture. Int J Dev Neurosci 2:247–257

Hansen GH, Wetterberg LL, Sjostrom H, Noren O (1992) Immunogold labelling is a quantitative method as demonstrated by studies on aminopeptidase N in microvillar membrane vesicles. Histochem J 24:132–136

Hommelgaard AM, Roepstorff K, Vilhardt F, Torgersen ML, Sandvig K, Van Deurs B (2005) Caveolae: stable membrane domains with a potential for internalization. Traffic 6:720–724

Miki T, Takegami Y, Okawa K, Muraguchi T, Noda M, Takahashi C (2007) The reversion-inducing cysteine-rich protein with Kazal Motifs (RECK) interacts with membrane type 1 matrix metalloproteinase and CD13/aminopeptidase N and modulates their endocytic pathways. J Biol Chem 282:12341–12352

Mineo C, Anderson RG (2001) Potocytosis. Histochem Cell Biol 116:109–118

Mu FT, Callaghan JM, Steele-Mortimer O, Stenmark H, Parton RG, Campbell PL, McCluskey J, Yeo JP, Tock EP, Toh BH (1995) EEA1, an early endosome-associated protein. EEA1 is a conserved alpha-helical peripheral membrane protein flanked by cysteine "Fingers" and contains a calmodulin-binding IQ motif. J Biol Chem 270:13503–13511

Nichols BJ (2002) A distinct class of endosome mediates clathrin-independent endocytosis to the golgi complex. Nat Cell Biol 4:374–378

Nichols BJ, Lippincott-Schwartz J (2001) Endocytosis without clathrin coats. Trends Cell Biol 11:406–412

Noda M, Takahashi C (2007) Recklessness as a hallmark of aggressive cancer. Cancer Sci 98:1659–1665

Nomura R, Kiyota A, Suzaki E, Kataoka K, Ohe Y, Miyamoto K, Senda T, Fujimoto T (2004) Human Coronavirus 229E binds to CD13 in rafts and enters the cell through caveolae. J Virol 78:8701–8708

Orlandi PA, Fishman PH (1998) Filipin-dependent inhibition of cholera toxin: evidence for toxin internalization and activation through caveolae-like domains. J Cell Biol 141:905–915

Ortegren U, Karlsson M, Blazic N, Blomqvist M, Nystrom FH, Gustavsson J, Fredman P, Stralfors P (2004) Lipids and glycosphingolipids in caveolae and surrounding plasma membrane of primary rat adipocytes. Eur J Biochem 271:2028–2036

Palade GE (1953) Fine structure of blood capillaries. J Appl Phys 24:1424

Parton RG (1994) Ultrastructural localization of gangliosides; GM1 is concentrated in caveolae. J Histochem Cytochem 42:155–166

Parton RG, Richards AA (2003) Lipid rafts and caveolae as portals for endocytosis: new insights and common mechanisms. Traffic 4:724–738

Parton RG, Simons K (2007) The multiple faces of caveolae. Nat Rev Mol Cell Biol 8:185–194

Patel HH, Murray F, Insel PA (2008) Caveolae as organizers of pharmacologically relevant signal transduction molecules. Annu Rev Pharmacol Toxicol 48:359–391

Pelkmans L, Burli T, Zerial M, Helenius A (2004) Caveolin-stabilized membrane domains as multifunctional transport and sorting devices in endocytic membrane traffic. Cell 118:767–780

Pelkmans L, Helenius A (2003) Insider information: what viruses tell us about endocytosis. Curr Opin Cell Biol 15:414–422

Pelkmans L, Zerial M (2005) Kinase-regulated quantal assemblies and kiss-and-run recycling of caveolae. Nature 436:128–133

Pelkmans L, Kartenbeck J, Helenius A (2001) Caveolar endocytosis of Simian Virus 40 reveals a new two-step vesicular-transport pathway to the ER. Nat Cell Biol 3:473–483

Pelkmans L, Puntener D, Helenius A (2002) Local actin polymerization and dynamin recruitment in SV40-induced internalization of caveolae. Science 296:535–539

Petrovic N, Schacke W, Gahagan JR, O'Conor CA, Winnicka B, Conway RE, Mina-Osorio P, Shapiro LH (2007) CD13/APN regulates endothelial invasion and filopodia formation. Blood 110:142–150

Riemann D, Kehlen A, Langner J (1999) CD13—not just a marker in leukemia typing. Immunol Today 20:83–88

Riemann D, Hansen GH, Niels-Christiansen LL, Thorsen E, Immerdal L, Santos AN, Kehlen A, Langner J, Danielsen EM (2001) Caveolae/lipid rafts in fibroblast-like synoviocytes: ectopeptidase-rich membrane microdomains. Biochem J 354:47–55

Riemann D, Tcherkes A, Hansen GH, Wulfaenger J, Blosz T, Danielsen EM (2005) Functional co-localization of monocytic aminopeptidase N/CD13 with the Fc gamma receptors CD32 and CD64. Biochem Biophys Res Commun 331:1408–1412

Sandvig K, Van Deurs B (2002) Membrane traffic exploited by protein toxins. Annu Rev Cell Dev Biol 18:1–24

Santilman V, Baran J, Nand-Apte B, Evans RM, Parat MO (2007) Caveolin-1 polarization in transmigrating endothelial cells requires binding to intermediate filaments. Angiogenesis 10:297–305

Schwachula A, Riemann D, Kehlen A, Langner J (1994) Characterization of the immunophenotype and functional properties of fibro-

blast-like synoviocytes in comparison to skin fibroblasts and umbilical vein endothelial cells. Immunobiology 190:67–92

Sharma DK, Choudhury A, Singh RD, Wheatley CL, Marks DL, Pagano RE (2003) glycosphingolipids internalized via caveolar-related endocytosis rapidly merge with the clathrin pathway in early endosomes and form microdomains for recycling. J Biol Chem 278:7564–7572

Simons K, Ikonen E (1997) Functional rafts in cell membranes. Nature 387:569–572

Styers ML, Kowalczyk AP, Faundez V (2005) Intermediate filaments and vesicular membrane traffic: the odd couple's first dance? Traffic 6:359–365

Tagawa A, Mezzacasa A, Hayer A, Longatti A, Pelkmans L, Helenius A (2005) Assembly and trafficking of caveolar domains in the cell: caveolae as stable, cargo-triggered, vesicular transporters. J Cell Biol 170:769–779

Thomsen P, Roepstorff K, Stahlhut M, Van Deurs B (2002) Caveolae are highly immobile plasma membrane microdomains, which are not involved in constitutive endocytic trafficking. Mol Biol Cell 13:238–250

Williams MA (1977) Quantitative methods in biology. In: Glavert AM (ed) Practical methods in electron microscopy. North-Holland/Elsevier, Amsterdam, pp 1–84

Williams TM, Lisanti MP (2004) The caveolin proteins. Genome Biol 5:214

Yamada E (1955) The fine structure of the gall bladder epithelium of the mouse. J Biophys Biochem Cytol 1:445–458